HIGH REDUNDANCY MULTIBEAM ECHOSOUNDER BACKSCATTER COVERAGE OVER STRONG RELIEF

Jean-Marie Augustin IFREMER, CS10070, 29280 Plouzané, France.
Jean.Marie.Augustin@ifremer.fr>
Geoffroy Lamarche NIWA, Private Bag 14-901, Wellington, 6241, New Zealand.
geoffroy.lamarche@niwa.co.nz

1 INTRODUCTION

After a very slow start and mostly from a research perspective, the interest from end-users (e.g. for offshore engineering, ocean science or environmental management) in the backscatter data co-registered with bathymetry by multibeam echosounder (MBES) is now growing. This is in part due to the potential for such data to help differentiate substrates based on sediment grain-size and heterogeneity and micro-topography[1]. Furthermore, backscatter data can provide quantitative information on the characteristics of seafloor substrates and micro-topography[2,3]. Today, industry and decision makers are starting to reap the benefit of backscatter-related technology in many engineering and environmental applications[4,5].

The backscatter signal recorded at the MBES receiving array is the result of complex physical phenomena, for which inversion in terms of geological features is not trivial nor unique[6]. One approach that bodes well for quantitative use of backscatter is the strong dependence of the Backscatter Strength (BS) on the incidence angle of the acoustic wave at the seafloor[4,7]. Unfortunately, over strong relief, incidence angles vary in non-trivial ways so that processing the resulting backscatter signal to produce meaningful and interpretable data is a complex and challenging undertaking.

Here we propose a unique approach, rarely undertaken, whereby MBES backscatter data are acquired along closely spaced transects, resulting in high overlaps between adjacent swaths and insonification of the seafloor target area by varying incidence angles. We use a MBES dataset purposefully collected on Brothers Volcano in the Kermadec volcanic arc, northeast of New Zealand (Fig. 1). The advantage of this site is its relatively simple outcropping geology (i.e., lava and volcano-sedimentary cover) and regional morphology, thus enabling us to concentrate on the impact of slope and substrate on the backscatter signal rather than on complex geological origins. The very steep morphology however prove at time problematic for this study.

The aim of the paper is to present this novel dataset and the potential that high redundancy data generated by strongly overlapping multibeam swaths provides in backscatter angular dependence studies. We focus on the specific processing made possible by the particular acquisition geometry, and address three issues: (1) the potential of filtering and stacking processes arising from the high-redundancy data, in particular with respect to speckle filtering and removal of the specular echo, without the inherent resolution loss that usually results from the use of traditional mosaicking algorithms; (2) the potential to generate equi-incidence angle backscatter mosaics, i.e. reflectivity maps composed of pixels originating from a narrow range of incidence angles; and (3) the potential to develop a supervised segmentation approach based on backscatter incidence angles for individual transects and the averaged image, thus providing a means to validate our supervised classification approach and methodology, whereby segmentations performed on individual transects should be comparable.

2 Data Acquisition

The bathymetry and backscatter dataset was acquired onboard RV *Tangaroa* over Brothers Volcano (34.87° S, 179.07° E) (Fig.1), which is the most hydrothermally active site within the Kermadec Arc[8]. The volcano edifice is 7x11 km at its base at ca. 2000 m water depth and is characterised by a ca. 3 x 3.4 km caldera, with its rim and floor lying at ca. 1500 m and 1800 m depths, respectively. A 600 m-high volcanic cone rises to 1200 m water depth in the SW quadrant of the caldera. The seafloor at Brothers Volcano consists of hard volcanic rocks, sometimes draped with soft fine-grained volcano-clastic sediments. This relatively simple surface geology provides a well-suited environment for our

study. The inner wall of the caldera is extremely steep with slopes often in excess of 40°, including a maximum value of 68° derived from a 10 m grid digital terrain model (DTM). A number of hydrothermal vents have been identified along the inner wall, essentially within the NW quadrant and the cone summits. The deepest part of the caldera floor, in the NW quadrant, is hummocky and likely consists of slump material originating from the neighbouring walls. Brothers Volcano has been the focus of intense research surveying as a potential site for deep-sea mining of Submarine Massive Sulphides (SMS), so the area is well documented with a large number of ground-truth data (sediment cores, camera images, rock dredges) that could be used to validate predictive maps (e.g., lithology,

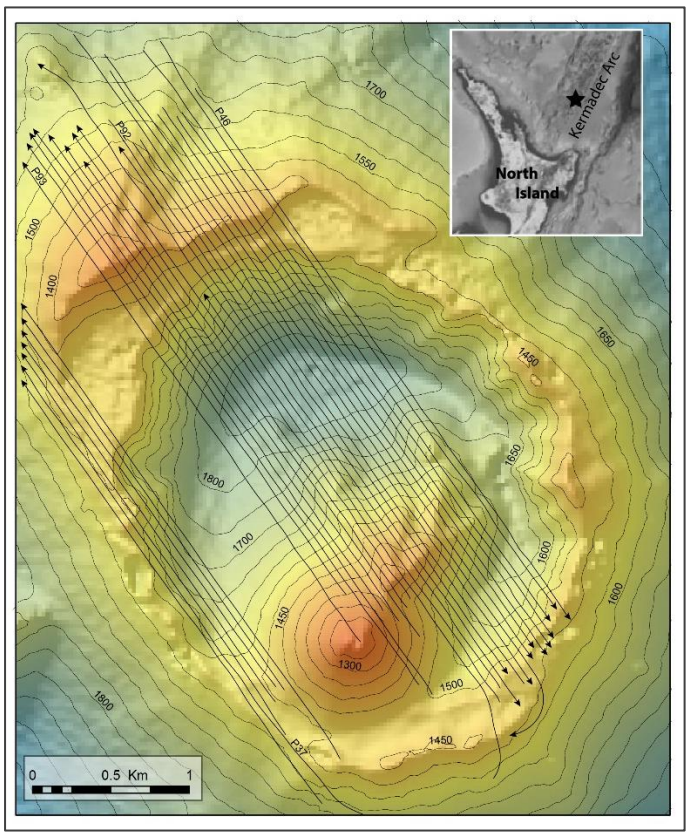

Figure 1 - Acquisition geometry in parallel multibeam transects across the Brothers Volcano, northeast of New Zealand. The lines shown used a 40° swath aperture and were run 50 m apart, interspersed by lines with a 5° swath aperture (not shown). The arrows show the direction of acquisition for parts of the lines. Insert: Location of the Kermadec arc and the Brothers Volcano (star). The profiles shown in Figs 5 and 6 are labelled.

benthic habitats, substrate).

The survey data presented here consists of a set of 60 parallel transects 25-m apart using a Kongsberg EM300 MBES. The swath aperture was set alternatively at 5° and 40° every second line (Fig. 2) and the system was run in "very deep" mode. A seismic streamer was towed for a simultaneous pseudo 3-dimensional seismic experiment, which required lines to be run in one direction only at a nominal speed of 5 knots. Because of poor weather conditions and limited sonar aperture, only 30 contiguous lines were available for the high swath-overlap experiment. A DTM with a 20-m grid was generated using the *Caris HIPS* software, later refined to 10 m using the *SonarScope* software of Ifremer[9].

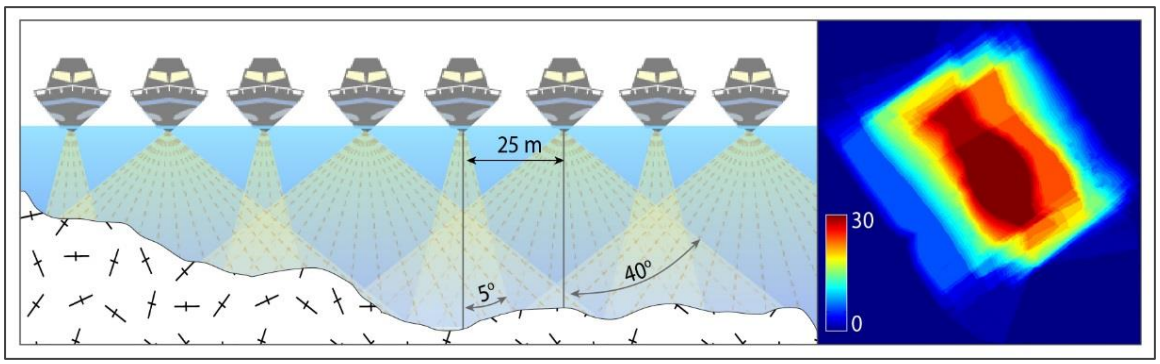

Figure 2 - Multibeam acquisition geometry (left) generating high swath overlaps with multiple incidence angle coverage. Right panel shows the redundancy achieved for each pixel, in number of pixel overlap.

Together with bathymetry, the EM300 co-registers backscatter data, i.e. the component of the sound signal strength that is reflected from the seafloor back to the vessel[10]. The backscatter relates to seafloor micro-topography (or roughness) and sediment volume heterogeneity, which in turn relates to sediment grain-size and composition[3]. Post-processing of the seafloor backscatter data (i.e. subsequently to data acquisition) was undertaken using *Sonarscope*[9]. Post-processing is required to remove artefacts attributable to the recording equipment and water column properties and to provide an interpretable image that can be used to quantify physical and geological parameters from the BS.

Our approach requires us to use BS values closest to the expected theoretical/physical values of the true angular backscatter. Hence, we only use data from the 40° swath aperture, as the 5° aperture does not provide information outside the specular echo. By default, with the EM300 system the backscatter data are automatically compensated at acquisition time for the effect of Lambert's Law, in order to flatten the backscatter decrease at grazing angles, and are corrected for the insonified area[6]. The post-processing specific to this experiment consisted of removing the effect of both compensations applied by the system, and reapplying an insonified area compensation using rigorously reassessed incidence angles. This required us to first carefully estimate the incidence angles of the backscatter acoustic waves on the seafloor in a true 3-dimentional context. The incidence angle is defined as the angle made between the direction of the acoustic wave when intersecting the seabed and line perpendicular to the seafloor. Such estimations are not trivial as they are highly dependent on the DTM used, in particular the grid size, and the type of filtering applied. Incidence angles calculated for a given area using DTMs with different levels of processing (e.g., gridding, filtering, smoothing) can show strong variations that directly affect the backscatter angular profiles (Fig 3 and 4). Here, we used a DTM generated from the averaging of co-located pixels. We thus obtained a satisfactory filtering of the bathymetric noise without the need for supplementary filters. This was made possible with this dataset due to the high-redundancy of co-located pixels, a process that is not achievable with data from traditional surveys, and in which case strong filtering is required. In particular, such an approach is essential for calculating true incidence angles.

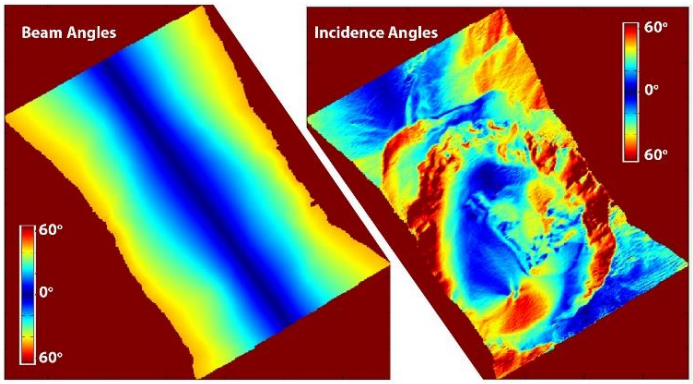

Figure 3 – Beam angles at the MBES array (left) and incidence angles at the seafloor (right) on Brothers Volcano. In an ideal flat seafloor configuration, the two images would be similar.

3 DATA PROCESSING

We present three procedures traditionally applied in backscatter studies which benefit substantially from the high redundancy of the seafloor incidence angle: (1) the generation of a backscatter mosaic free of speckle noise and specular echo; (2) the building of equi-incidence angle mosaics; and (3) the segmentation of backscatter data using their incidence angle profiles for classification purposes.

The speckle noise is a phenomenon particularly present in sonar images (Figs 4 and 5); it is not instrument-related but is rather inherent to the physical interaction of the acoustic waves with the seafloor. Speckle filtering is usually undertaken at the final stage of backscatter processing by applying a nearest-neighbour weighted filter[10]. This approach systematically results in some loss of sharpness in the final image. In our study, the high data redundancy makes it possible to stack co-

located, overlapping, pixels, resulting in a substantial attenuation of the speckle noise, without resolution loss. The averaging includes backscatter data from individual transects generated with incidence angles greater than 12°, i.e. excluding the specular echo (Fig. 5 bottom right). The 12° threshold was chosen from an estimate of the average width of the specular echo on the angular profiles. To create the average reflectivity image, all the backscatter data generated from incidence angles less than 12° were masked. The final mosaic was created using a grid size of 10 m.

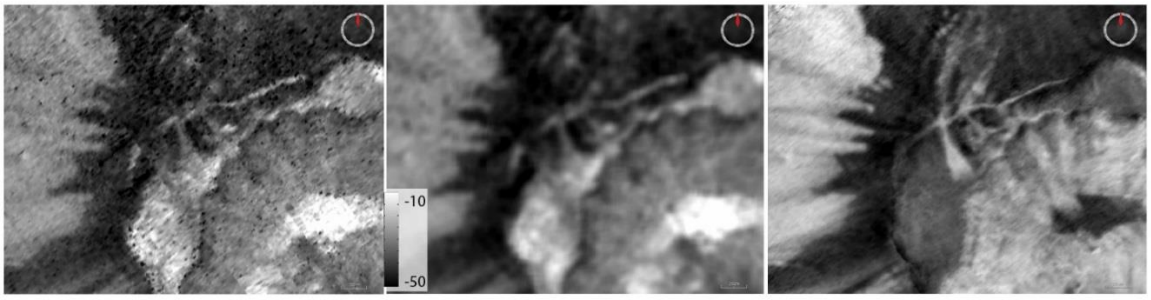

Figure 4 – Mosaics before (left) and after (right) averaging of co-located pixels. The central image shows a traditional Wiener filtering applied to the left image for comparison.

The averaged backscatter mosaic presents two substantial advantages compared to those traditionally generated from swath surveys[4] (Fig. 5). First, the specular echo, which most often completely overshadows parts of the mosaics, has efficiently been removed; and second, the image has a similar appearance as after traditional speckle filtering. We believe, however, that the sharpness of the final image has increased compared to traditional speckle filtering (see discussion), and that such mosaics (that do not have the specular echo) are better suited for interpretation, segmentation and generation of seafloor habitat and substrate classification maps (Figs 4 and 5, bottom right).

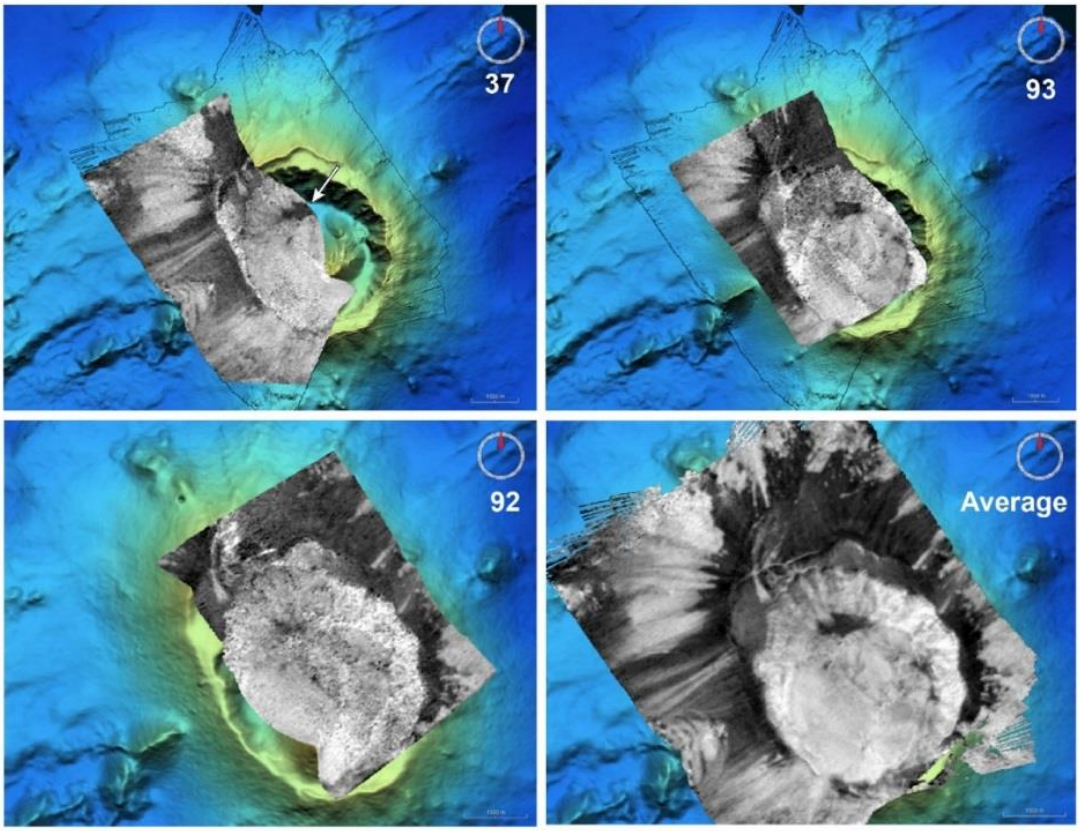

Figure 5 - Individual swath profile numbers 37, 93 and 92 over Brothers Volcano (location on Fig. 1), and the averaged mosaic (bottom right panel). All frames have the same geographic coverage. The white arrow on the top left map shows the location that appears with differing reflectivity on profile 92 (see text).

Such a dataset makes it possible to generate a variety of backscatter mosaics at different incident angles. We first generated five mosaics using backscatter data from incidence angle sectors, each spanning 15°, from 0-15° to 60-75° (Fig. 6 - right). These 10 m grid mosaics were generated by masking any data taken at incidence angles outside the desired sector. This approach, however, results in data gaps in the mosaics where incidence angles are out of the selected angle sector. Some gaps in the examples shown here may also originate from poor weather conditions during which data acquisition was interrupted (Fig. 1), and from the lack of data for incidence angles lower than the along-track slope, a phenomenon often observed for steep along-track slopes.

Finally, a procedure of supervised data segmentation developed by Dugelay et al.[11] was applied to our dataset. The method is based on the BS variations with seafloor incidence angle; the pixels are assigned to the class with the shortest statistical distance between locally-measured reflectivity and a set of given Gaussian density functions defined by angular BS profiles and their standard deviations (Fig. 7 - left). In traditional supervised segmentation, regions of interest (known as training regions) are first selected by the user, based on a visual interpretation of the backscatter mosaic[4], defining a small number of classes. Here, we selected two main classes using a threshold of the average level at -35 dB (Fig. 7); these classes were defined from the BS2 and BS4 angular profiles. BS2 is computed as the average of all BS profiles over Brothers Volcano for values greater than -35 dB. BS4 is the average of all BS profiles for values lower than -35 dB. Five classes were finally defined based on BS2 and BS4. Classes 2 and 4 are defined by the values either sides of the BS2 and BS4 angular profiles, bounded by their respective standard deviations; hence, pixels assigned to classes 2 and 4 show statistical properties close to the corresponding training regions. Class 1 is defined by pixel values higher than (BS2+std2), while Class 5 is defined by pixels with values that are lower than (BS4-std4). Finally, the intermediate Class 3 includes pixel values falling between (BS4+std4) and (BS2-std2).

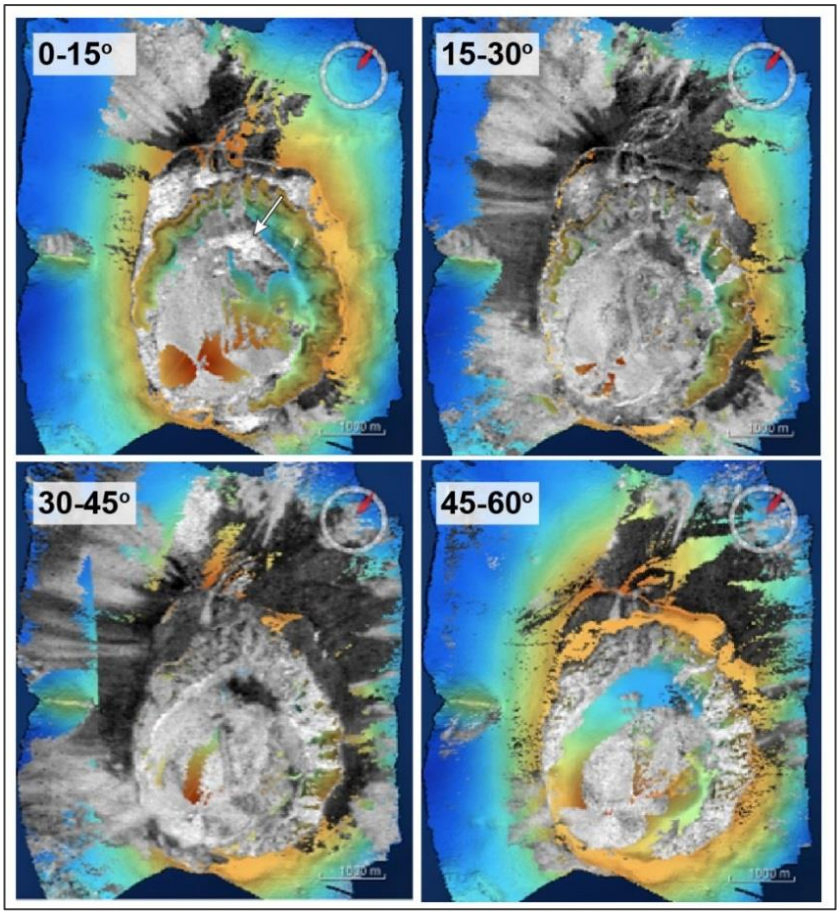

Figure 6 - Mosaics for four sectors of incidence angles (0-15°, 15-30°, 30-45° and 45-60° (60-75° not shown)). Backscatter data are represented using a grey level scale and superimposed on coloured bathymetry. Data gaps where coloured bathymetry shows inside the backscatter image occur either when no data with the required angle were recordered or where no data were recorded at all.

Once all the pixels were assigned to a class, we generated classification maps for individual swaths (Fig. 8). Finally, we combined all individual segmented data into synthetic classification maps for the Brothers Volcano, where every pixel value is the median value of all co-located pixels of the individual segmented swaths.

4 DISCUSSION

The prime advantage of this dataset is the insonification of a given seafloor target area by multiple incidence angles. The final backscatter image (Fig. 5 - bottom right), generated from averaged co-located pixels and masking of incidence angles smaller than 12°, offers three obvious benefits compared to traditionally processed images. First, it is free of MBES contributions of the specular echo that plague classical sonar images. Note that transmit-sector artefacts, often visible in traditional data are also removed. Second, the multi-layer stacking very effectively attenuates the speckle noise. Whilst in traditional post-processing, speckle filtering usually results in a loss of resolution, here details are preserved and possibly improved compared to the former stage of the image (Fig. 4). Third, noise reduction actually increases the image contrast since the resulting BS-value histogram is narrower than that of the unfiltered image. Overall, the stacked mosaic (Fig. 4 right) shows enhanced depiction of fine features, and sharper boundaries between backscatter facies. Before averaging co-located pixels, mosaics display regions of very high backscatter intensity, suggesting that the specular echo is dominating the signal, which is readily confirmed by checking the incidence angles. Thus, the averaging of all swath contributions and masking of the specular echo provides a much clearer image.

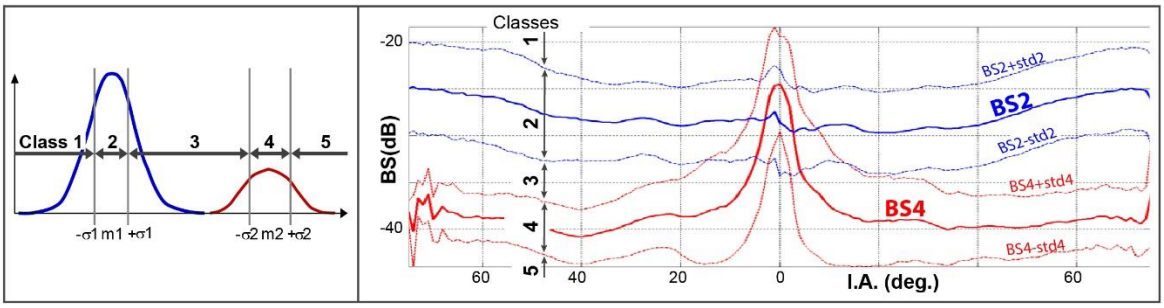

Figure 7 – Backscatter angular profiles (right) for incidence angles greater (blue) and lower (red) than -35° dB with standard deviations (dashed lines). Left: Probability density function of the backscatter angular profiles given here by their average values (m_1 and m_2) at -45°incidence angles, with their standard deviations (σ_1 and σ_2). Right: The five segmentation classes (illustrated by the vertical arrows) are defined by statistical distances from the distributions BS2 and BS4 (left), as well as the outside and intermediate statistical ranges of the BS values.

The classification map (Fig. 8) is largely dominated by classes 2 and 4. Class 2 is defined by high reflectivity and covers the inner wall of the caldera including the volcanic cone and the outer base of the edifice. This suggests that this class relates to steep slopes and hard, rough seafloor, possibly corresponding to outcropping lava. Class 4 characterises a low reflectivity facies and covers most of the outer flank of the edifice and the flat floor of the caldera. This suggests there is soft material at the seafloor, most likely volcano-clastic material draping the volcano flanks as observed by other geological studies on Brothers Volcano[8,12]. Class 4 on the caldera floor may indicate remobilised material from the caldera wall as suggested by photos and samples[8]. Class 1 is characterised by the highest reflectivity level, is very limited geographically and has little coherency. It is observed essentially along the inner caldera wall, possibly suggesting very steep slopes or rough, outcropping lava, and towards the base of the NW quadrant of the edifice, where it could be related to downslope accumulations of coarser volcano-clastic material. Class 5 has the lowest reflectivity and also limited geographical extent, but displays much better defined patches than class 1. Well defined patches of class 5 are observed along the caldera inner flank where high hydrothermal activity has been observed[12], an interesting relationship that may prove beneficial to investigate further, and at the base of the northern part of the volcanic edifice.

The dataset also provides a means to study the backscatter signal dependence on incidence angles at the seafloor. On the mosaics generated using narrow incidence angle sectors, some areas display contrasting BS values from one range of incidence angles to the other. A particular example is the caldera floor (e.g. white arrow on Figs 5 and 6), which displays very low reflectivity on swaths 37, 93 and the averaged mosaic, but high reflectivity on swath 92. This shows that some geological features may return rather differing BS depending on the incidence angle of the insonifying acoustic wave. Interestingly in this particular case, the floor of the caldera is flat and likely to consist of remobilised fine sediment, possibly suggesting SMS mounds. Such an interpretation, which needs validation, would provide very beneficial information for deep-sea mining resources research. The outer flank of the volcanic edifice is characterised by low reflectivity and the inner wall shows high reflectivity, observations that would be expected from the known geology of the volcano[8].

Reflectivity maps where the whole area is insonified, according to one narrow incidence angle sector (Fig. 6), are substantially different from previous approaches where non-overlapping swaths implied that angular responses at high and low angles could correspond to different substrates. The multi-angle mosaics illustrate clearly the difficulty of interpreting sonar images produced from traditional surveys over steep slopes. Ideally, backscatter post-processing would remove all slope effects so that it would only relate to the substrate. This is a very complex undertaking, which requires subtracting the angular backscatter value (as read on the BS profile) for the corresponding class, and reapplying the mean BS value for that class. For instance, BS4 at 45° on Figure 7 has a value of -45 dB and the mean value for BS4 is ca. -38 dB, so that the correction would be ca. 7dB. Here, we have generated a segmentation map that indexes the angular BS, but stops short of applying the final correction of the angular BS corresponding to the class identified for that pixel.

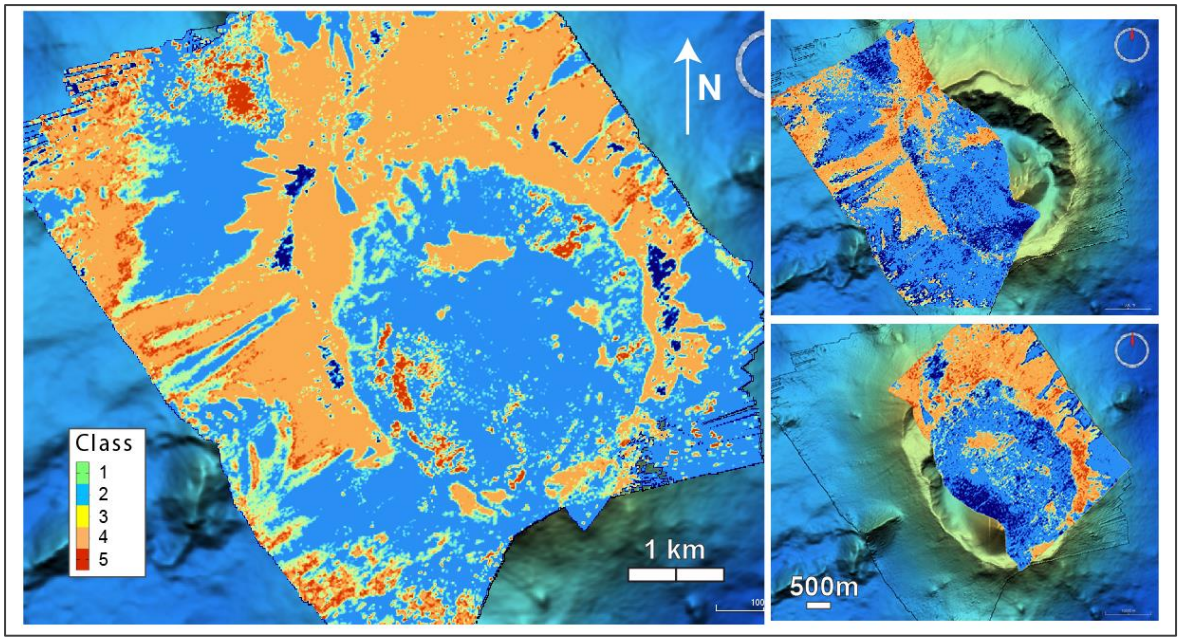

Figure 8 - Segmentation and classification using the five classes (Fig. 7) defined from the statistical distance from the mean backscatter angular value. The right panels show segmentation results on two individual swaths (two extreme profiles on Fig. 1). Other individual swath segmentations are available at https://forge.ifremer.fr/docman/?group_id=126&view=listfile&dirid=505

Overall, the segmentation procedure that we applied to the 30 MBES transects across Brothers Volcano produces coherent results. This image processing technique is based on a determinist algorithm that analyses the BS with respect to the incidence angle. This results in an image that is readily interpretable. The fact that these results are similar for every overlapping transects demonstrates that the upstream processing sequence is valid; in particular: (1) our estimation of the incidence angles are correct; and (2) the compensation for the insonified area is properly reapplied. Very importantly, this validates the procedures generally applied after conventional backscatter surveys for which such cross-validations are not available.

5 CONCLUDING STATEMENT

This experiment demonstrates the potential of dedicated surveys with highly overlapping swaths from running closely-run, parallel transects. Unfortunately, it is limited to dedicated surveys where parallel survey tracks are run with close spacings, which indeed is perceived as inefficient and expensive compared to traditional bathymetry surveys. Importantly, our experiment seems to support traditional processing sequences and interpretation of MBES and backscatter data.

Surveys dedicated to backscatter data are still uncommon, but based on the success of this experiment, applications such as predictive mapping of marine resources and seafloor habitats using remotely-sensed MBES data would benefit from further R&D. Should further similar surveys be undertaken, care needs to be taken to: (1) use a wider sonar aperture, since the limitation at 40° in our experiment obviously limited the extent of the results; (2) optimise the amount of overlap. This is indeed dependent on the water depth. In our study, 50 m line-spacing provided an excellent mean to demonstrate the potential of the approach but did not provide sufficient data redundancy over the entire volcanic edifice. It shallower water depths, the line spacing will most need to be smaller; (3) run lines in alternate directions so that the local backscatter is recorded alternatively by starboard and port beams; and (4) acquire cross-lines, or in a star-like geometry, to increase variations in insonification direction at the seafloor and help minimise the gaps in incidence angles. Obviously, these suggestions require careful planning[10] and must be balancing with funding, time and logistical requirements.

ACKNOWLEDGMENT

The authors wish to thank Xavier Lurton (Ifremer) and Arne Pallentin and Scott Nodder (both NIWA) for reviewing this paper.

REFERENCES

1 de Moustier, C. (1986) Beyond bathymetry: mapping acoustic backscattering from the deep seafloor with Sea Beam. *J. Acoustic. Soc. Am.*, 79: 316-331.

2 Brown, C. J. & Blondel, P. (2009) Developments in the application of multibeam sonar backscatter for seafloor habitat mapping. *Appl. Acoust.*, 70: 1242-1247.

3 Jackson, D. R. & Briggs, K. B. (1992) High-frequency bottom backscattering: Roughness versus sediment volume scattering. *J. Acoustic. Soc. Am.*, 92: 962-977.

4 Lamarche, G., Lurton, X., Verdier, A.-L. & Augustin, J.-M. (2011) Quantitative characterization of seafloor substrate and bedforms using advanced processing of multibeam backscatter. Application to the Cook Strait, New Zealand. *Cont. Shelf Res.*, 31: S93-S109.

5 Lucieer, V. & Lamarche, G. (2011) Unsupervised fuzzy classification and object-based image analysis of multibeam data to map deep water substrates, CookStrait, New Zealand. *Cont. Shelf Res.*, 31: 1236-1247.

6 Lurton, X. (2010) *An Introduction to Underwater Acoustics. Principles and Applications. 2nd edition*. Springer Praxis Books & Praxis Publishing, UK: 346.

7 Hughes Clarke, J. E., Danforth, B. W. & Valentine, P. (1997) Areal seabed classification using backscatter angular response at 95 kHz. *High Frequency Acoustics in Shallow Water, NATO SACLANT Undersea Research Centre*, Lerici, Italy, 30 Jun-4 Jul 1997.

8 Embley, R. W., de Ronde, C. E. J., Merle, S. G., Davy, B. & Tontini, F. C. (2012) Detailed Morphology and Structure of an Active Submarine Arc Caldera: Brothers Volcano, Kermadec Arc. *Economic Geology*, 107: 1557-1570.

9 Augustin, J. M. & Lurton, X. (2005) Image amplitude calibration and processing for seafloor mapping sonars. *Oceans 2005 - Europe*, 20-23 June 2005. Vol.1: 698 - 701. 10.1109/OCEANSE.2005.1511799

10 Lurton, X. & Lamarche, G. (2015) Backscatter measurements by seafloor-mapping sonars. Guidelines and Recommendations. Joint IHO - Geohab Report. , 200p.

11 Dugelay, S., Graffigne, C. & Augustin, J. M. (1996) Deep seafloor characterization with multibeam echosounders by image segmentation using angular acoustic variations. Proceedings SPIE's 96, Denver, August 1996 Vol.2823: 255-266.

12 De Ronde, C.E.J., Hannington, M.D., Stoffers, P., Wright, I.C., Ditchburn, R.G., Reyes, A.G., Baker, E.T., Massoth, G.J., Lupton, J.E., Walker, S.L., Greene, R.R., Soong, C.W.R., Ishibashi, J., Lebon, G.T., Bray, C.J. and Resing, J.A. (2005) Evolution of a submarine magmatic-hydrothermal system: Brothers volcano, southern Kermadec Arc, New Zealand. Economic Geology, 100(6): 1097-1133.